International Journal of Automotive Technology, Vol. 6, No. 3, pp. 205–213 (2005)

1229–9138/2005/021–02

NUMERICAL MODEL ON THE FUEL INJECTION CHARACTERISTICS FOR PREDICTING EXHAUST EMISSIONS FROM A MARINE DIESEL ENGINE

S.-Y. LEE, G.-B. KIM, C.-H. JEON* and Y.-J. CHANG

Department of Mechanical Engineering, RIMT, Pusan National University, Busan 609-735, Korea

(Received 3 March 2004; Revised 5 October 2004)

ABSTRACT–This study deals with the result of exhaust emissions and performance calculated by simulation of the fuel injection characteristics of the inline injection system in a marine diesel engine. The emissions are calculated through non-equilibrium by using the extended Zel'dovich kinetic mechanism for NOx and equilibrium method for OH, CO, H_2, H and soot concentrations. Comparisons of the model predictions with the experimental values show reasonable agreement. Detailed prediction results showing the sensitivity of the model by injection rates are presented and discussed.

KEY WORDS : Fuel injection characteristics, Injection rate, Non-equilibrium, Zel'dovich kinetic mechanics

NOMENCLATURES

A	: area
C	: model constant
D	: diameter of high pressure pipe
F	: initial force
K	: bulk modulus of fuel oil
P	: pressure
Q	: heat value
R	: radius
Re	: reynolds number
U	: velocity
V	: volume
a	: R. S. Dow's constant
b	: C. E. Fink's constant
c	: velocity of wave propagation
f	: Darcy-Weisbach friction facter
g	: gravitational constant
k	: stiffness of spring
m	: mass
t	: time
x	: displacement
ρ	: fuel density
ρ_0	: fuel density under standard temperature and atmosphere
t	: time
θ	: angle
λ	: damping coefficient

**Corresponding author.* e-mail: chjeon@pusan.ac.kr

SUBSCRIPTS

bf	: burned fuel
cyl	: combustion chamber
e	: cavitation
f	: fuel
fv	: fuel vaper
g	: gas
h	: nozzle hole
id	: ignition delay
l	: high pressure pipe
liq	: liquid
n	: needle
no	: area of nozzle valve opening
o	: oxygen
s	: soot
sc	: sac chamber
so	: soot oxidation
sp	: spill port
u	: plunger
v	: constant volume
vap	: vapor

1. INTRODUCTION

The performance of a diesel engine and its resulting exhaust emission compositions depend on the injection rate, the injection pressure and the injection duration of the supplied fuel. The fuel injection characteristics dominate the combustion process within a combustion chamber; hence, it is important to determine those

characteristics that are closely related to fuel injection, namely combustion performance and exhaust emissions. There have been various studies aimed at raising diesel engine efficiencies while decreasing noxious emissions by optimizing the fuel injection system. Among the numerous studies on fuel injection systems (Mastuoka, 1976; Kumar, 1983; Wylie *et al.*, 1971; Becchi, 1971), studies concerning marine engine injection systems have been lacking, especially on the resulting impact of changes in injection pipe size, retraction volume, plunger area, pump and motor speed, plunger chamber cam configuration, etc.-factors that affect the performance of the fuel injector. The present research takes the above into account when calculating the injection characteristics of a marine engine fuel injection system with alternating variables; these results in turn are used to calculate fuel mass burn rate and calculate the exhaust emissions that include factors for *NO*, *CO* and *soot* ultimately. It is hoped that the results will contribute towards future engine development.

2. THEORETICAL ANALYSIS

2.1. Fuel Injection Model

2.1.1. Continuity equation in the plunger chamber

The pressure change of the plunger chamber depends on the following: The change in volume, A_uU_u, due to plunger movement; the volume of fluid drained through the spill port, $C_{SP}A_{SP}\sqrt{2/\rho[P_u-P_{sp}]}$; and the volume of fluid sent to the injection pipe, A_lU_l.

The relationship between the three is as shown in equation (1).

$$\frac{dP_u}{dt}=\frac{K_u}{V_u}\left(A_uU_u-C_{sp}A_{sp}\sqrt{\frac{2}{\rho}[P_u-P_{sp}]}-A_lU_l\right) \tag{1}$$

2.1.2. Fuel injection nozzle

Continuity Equation in the Nozzle Chamber

The pressure change within a nozzle depends on the following: The fluid from the injection pipe, A_lU_l; the volume displacement, A_nU_n, due to the nozzle needle valve movement; and the volume discharging to the sac chamber $C_nA_{no}\sqrt{2/\rho[P_n-P_{sc}]}$. The relationship between the three is as shown in equation (2).

$$\frac{dP_n}{dt}=\frac{K_n}{V_n}\left(A_lU_l-A_nU_n-C_nA_{no}\sqrt{\frac{2}{\rho}[P_n-P_{sc}]}\right) \tag{2}$$

Momentum Equation of the Nozzle Needle Valve

Momentum of the needle valve, mass m_n, depends on the following: Force due to the pressure in the nozzle chamber, $(A_n-A_{sc})P_n$; force due to the pressure from the sac chamber, $A_{sc}P_{sc}$; the needle valve spring force, F_n, which controls the nozzle opening; the reduction of force between the needle valve and the nozzle housing λ_nU_n; and the force in the spring, K_nx_n, due to changes in needle valve position. The relationship between the five is as shown in equation (3).

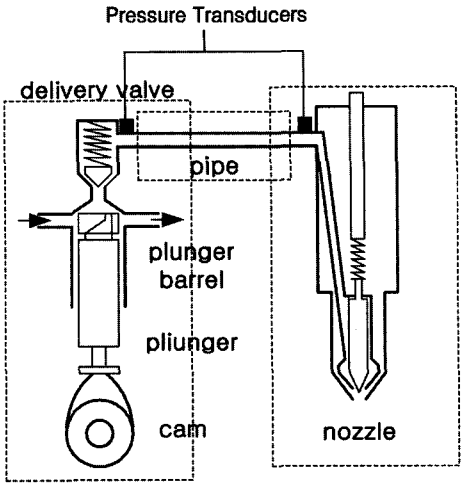

Figure 1. Schematic illustration of injection system.

$$\frac{dU_n}{dt}=\frac{1}{m_n}((A_n-A_{sc})P_n+A_{sc}P_{sc}-F_n-k_nx_n-\lambda_nU_n) \tag{3}$$

Continuity Equation within the Sac Chamber

Equation (4) represents change in fuel injection volume due to the pressure difference between the nozzle chamber and the needle sac, and the pressure differential between the needle sac and the combustion chamber.

$$\frac{dP_{sc}}{dt}=\frac{K_{sc}}{V_{sc}}\left(C_nA_{no}\sqrt{\frac{2}{\rho}[P_n-P_{sc}]}-C_hA_h\sqrt{\frac{2}{\rho}[P_{sc}-P_{cyl}]}\right) \tag{4}$$

2.1.3. Fuel injection pipe

It was assumed that the flow within the fuel injection pipe was one-dimensional unsteady flow. Furthermore, taking into account the compressible flow and frictional losses within the pipe, the following non-linear partial differential equations for the momentum equation and the continuity equation can be obtained.

$$L_1=\frac{\partial P}{\partial x}\rho+U\frac{\partial U}{\partial x}+\frac{\partial U}{\partial t}+\frac{fU|U|}{2D}=0 \tag{5}$$

$$L_2=U\frac{\partial P}{\partial x}+\frac{\partial P}{\partial t}+\rho c^2+\frac{\partial U}{\partial x}=0 \tag{6}$$

The friction coefficient in the pipe is represented by f.

The friction term $fU^2/2D$ in the momentum equation operates inversely to the flow direction; hence it must be represented as $fU|U|/2D$. If a characteristic curve is obtained from the above partial differential equations and converted into ordinary differential equations, we can obtain the following ordinary differential equations.

$$\frac{dU}{dt}+\frac{1}{\rho a}\frac{dP}{dt}+\frac{fU|U|}{2D}=0 \tag{7}$$

$$\frac{dx}{dt} = U + a \tag{8}$$

$$\frac{dU}{dt} - \frac{1}{\rho a}\frac{dP}{dt} + \frac{fU|U|}{2D} = 0 \tag{9}$$

$$\frac{dx}{dt} = U - a \tag{10}$$

Equations (7) to (10) are characteristic curves which exist on the x–t plane (Kumar, 1983). Equation (7) is true if and only if equation (8) is true. Likewise, equation (9) is true if and only if equation (10) is true. Flow velocity, U, is a function of distance, x, so flow velocity appears as a curve within the x–t plane. Moreover, the equation of $\Delta t/\Delta x$ must satisfy the following requirement to assure stability.

$$\Delta t(U + c) \leq \Delta x \tag{11}$$

If the above equations are applied to the injection pipe, it becomes possible to find the flow volume and pressure at any point within the pipe. The pressure and flow at either ends of the injection pipe can be obtained by setting the appropriate boundary conditions and through the characteristic curves.

2.1.4. Physical properties and coefficients

Fuel Properties, Density and Bulk Modulus

$$\rho = \rho_0(1 + aP - bP^2) \tag{12}$$

$$K = -V\frac{\partial P}{\partial V} = \frac{1 + aP - bP^2}{a - 2bP} \tag{13}$$

The fuel properties are shown in Table 1. ρ_0 is the fuel density under standard atmospheric temperature, while "a" and "b" represent R.S. Dow and C.E. Fink's constants (Dow *et al.*, 1940).

Coefficient of Friction within the Pipe

Fluid friction due to viscosity, f, is proportional to speed, and is applied via the Darcy-Weisbach equations as in the following.

Table 1. Fuel composition.

Molecular formular	$C_{14.4}H_{26.2}$
Specific gravity at 15°C	0.8296
Viscosit at 40°C	2.7
LHV, kcal/kg	10,266
Cetane #	46.2
Hydrogen, % mass	13.12
Carbon, % mass	86.62
Nitrogen, % mass	0.022
Sulfur, % mass	0.038
Oxygen, % mass	0.

Laminar field : $f = \frac{64}{\mathrm{Re}}$ (14)

Transient field : $f = 0.00019064\mathrm{Re}^{0.64378}$ (15)

Turbulent field : $f = 0.3164\mathrm{Re}^{-0.25}$ (16)

Cavitation

In the event of cavitation, density and bulk modulus are represented as ρ_e and K_e, and are calculated as follows (Wylie *et al.*, 1971; Becchi, 1971).

$$\rho_e = \rho_i + \frac{\Delta M}{V} \tag{17}$$

$$K_e = \frac{K_{vap}}{1 + [(K_{vap} - K_{liq})/K_{liq}]/Vx} \tag{18}$$

$$Vx = \frac{\rho_{liq} - \rho_e}{\rho_{liq} - \rho_{vap}} \tag{19}$$

2.1.5. Algorithm

In order to obtain accurate numerical values of the overall fuel injection system, fourth order Runge-Kutta schemes were applied to four differential equations at the pump and nozzle ends. The method of characteristics was used on the two partial derivatives of the fuel injection pipe.

2.1.6. Determination of coefficient constants

In other to calculate flux at the position of chamber gates, all sections were assumed to be orifice system and orifice equations were applied. The flux in orifice system is determined by fluid velocity, geometric sectional area and flux coefficients. According to researcher, the flux coefficient constants in orifice system are not same and the constants of 0.6–0.7 are applied normally. In this study, nozzle hole was applied to constant of 0.7, and nozzle needle and spill port were applied to constant of 0.64 and 0.67 respectively.

2.2. Combustion Model

Combustion was assumed to be one-zone and the ignition delay time, -the period between fuel injection into the cylinder and ignition itself-was obtained using the following equation (Hiroyasu, 1989).

$$\tau_{id} = 0.0405P_{cyl}^{-0.757}\exp\left(\frac{5473}{T_{cyl}}\right) \tag{20}$$

Mass burn-rate was defined as in equation (21) (Whitehouse *et al.*, 1969; bazari, 1992),

$$\dot{m}_{bf} = 5 \times 10^{10}\rho_g^2[fuel][O_2]^5\exp\left(\frac{-12000}{T_{cyl}}\right) \tag{21}$$

And the fuel mass that went through combustion was limited by the amount vaporized. The equation below was used to calculate heat loss.

$$Q_{loss} = HA(T_{cyl} - T_{wall}) \quad (22)$$

$$H = 0.99(3.5 + 0.185C_{loss})(P_{cyl}^2 T_{cyl})^{\frac{1}{3}} \quad (23)$$

To obtain the temperature of the gas in the cylinder, the results from the above equations were used to solve the equations below.

$$mdu = dQ_{fuel} - dQ_{loss} - P_{cyl}dV_{cyl} \quad (24)$$

$$du = C_v dT_{cyl} \quad (25)$$

2.3. Exhaust Model

In a diesel engine, CO_2, O_2, H_2O, and N_2, compromise the majority of the exhaust, followed by *NO* and *soot*, depending on the pressure and temperature. *CO* is generally not a major component of diesel exhaust. The gas components CO_2, O_2, H_2O, and N_2, have a relatively short reaction time as compared to the combustion time, and were calculated using equilibrium equations. *NO*, however, takes a long time to reach equilibrium and was calculated using non-equilibrium equations.

The Zeldovich mechanism, the process of converting atmospheric nitrogen into *NO*, was used for the *NO* calculations in the combustion model. This mechanism is the most appropriate mechanism to apply to standard fuel-air mixtures in the combustion chamber. Moreover, the degree of fuel-air mix-ratio differs depending on the location in the combustion chamber. Some researchers divide the combustion chamber into multiple zones in order to calculate emissions in the separate zones, and then average the results. In the current research, however, the exhaust was calculated under a model that assumes a homogeneous mixture in the combustion chamber, and that the chamber has one zone. To calculate the concentration of *soot*, the following equation was used (Hiroyasu *et al.*, 1989). Where the coefficient constant of C_f and C_s and were applied to 35 and 21120 respectively.

$$dm_s = C_f m_{fv} P_{cyl}^{0.5} \exp\left(\frac{-E_f}{RT_{cyl}}\right) - C_s m_s \frac{P_0}{P_{cyl}} P_{cyl}^{1.8} \exp\left(\frac{-E_s}{RT_{cyl}}\right) \quad (26)$$

3. EXPERIMENTAL SETUP

The engine used to conduct the research was a 4-stroke diesel engine used in vessels. The specifications for the engine are shown in Table 2. The main experimental equipments are the dynanometers, to measure and control engine torque; the mass flow meter, to measure the consumption of fuel; and the exhaust analyzer,to measure concentration levels of *NOx*, CO_2, O_2, and *soot* in the emissions. And the stardard operating condition are shown in Table 3.

Table 2. Specifications of engine and injection system.

Combustion system	Direct injection
Air supply type	Turbo charger
Displacement volume (cc)	19694
Compression ratio	13.3
Power (kW)	1890
Max. comb. pressure (bar)	128.8
Injection system	Jerk's method
Nozzle hole diameter (mm)	0.32
Number of nozzle hole	8
Angle between nozzle hole (degree)	145°

Table 3. Standard operating conditions.

Intake air temperature (K)	319
Intake air pressure (kPa)	104.4
Cylinder wall temperature (K)	473
Engine speed (rpm)	775
Injection timing (degree)	−13° ATDC
Nozzle opening pressure (bar)	320
Plunger effective stroke (mm)	3.75
Pre-stroke (mm)	7

4. RESULTS AND DISCUSSION

Figure 2 shows the result of the numerical analysis and the experimental result. Note the two results are extremely similar. Figure 3 shows the result of the numerical analysis, which are pressure in injection pipe, delivery and nozzle lifts.

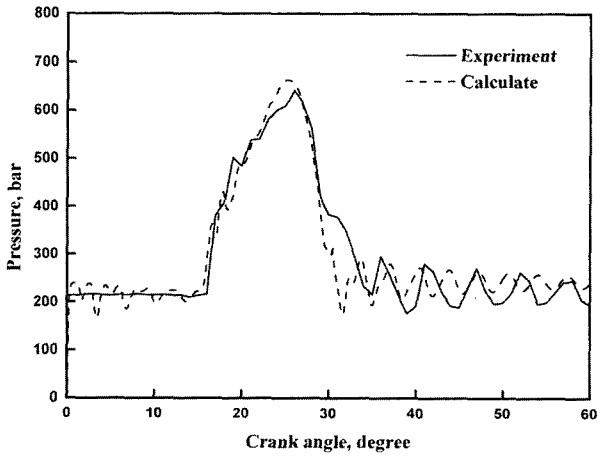

Figure 2. Comparison for experiment and calculated result at the end of injection pipe.

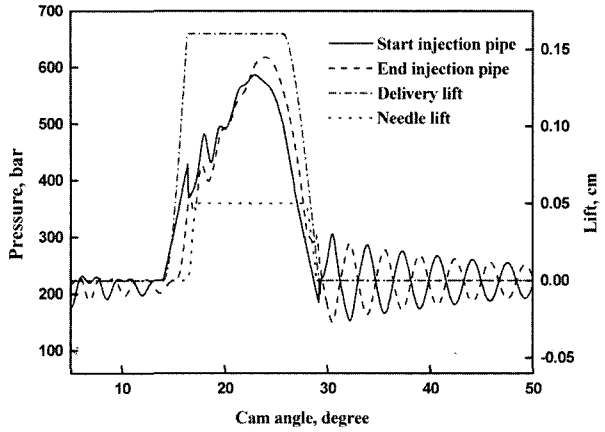

Figure 3. Result of injection system simulation.

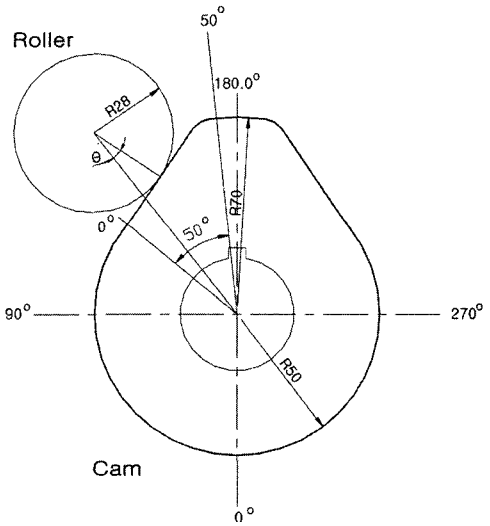

Figure 4. Cam configuration.

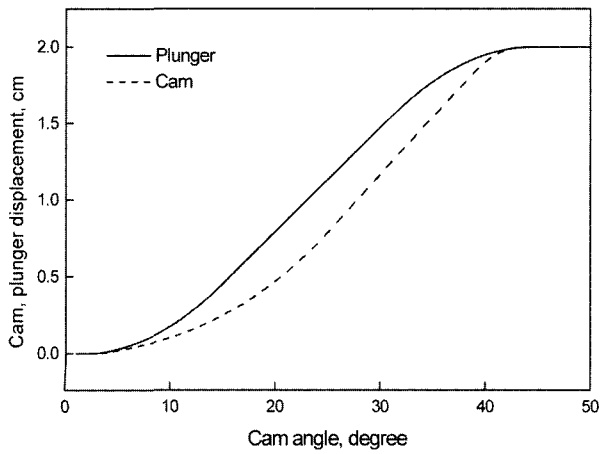

Figure 5. Cam and plunger displacement for standard cam.

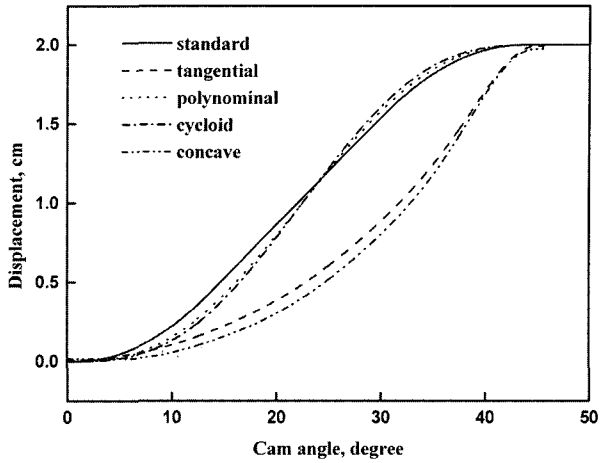

Figure 6. Plunger displacement for cam profile.

Figures 4 and 5 show the cam configuration and correlation between cam and plunger displacement which calculated by equations (27) to (29) for stanard cam.

$$x_{roller} = x_{plunger} + R_{cam} \tag{27}$$

$$= \frac{R_{roller}}{\cos\theta} - R_{cam} + x_{cam} \tag{28}$$

$$= R_{roller}\left(\frac{1}{\cos\theta} - 1\right) + x_{cam} \tag{29}$$

Figure 6 shows the result of plunger displacement as related to changes in the cam profile. The cam profile was changed to calculate the characteristics of the systemunder identical displacement and displacement duration for tangential, polynomial, cycloid, and concave cams, and compared to the system's actual standard cam. Figures 7 and 8 are examples of module variables that affect the system's characteristics. Figure 7 shows the effect of changes in pump plunger area. It is theorized

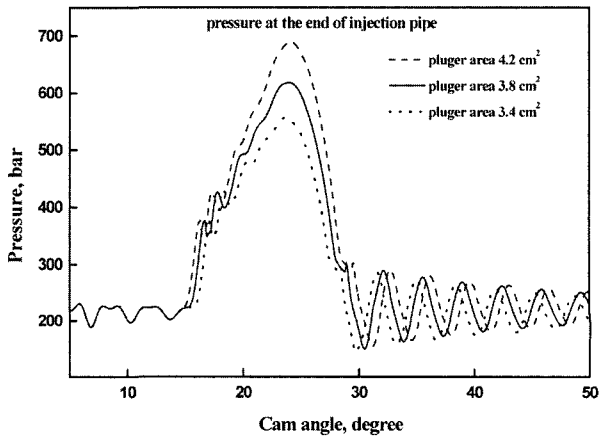

Figure 7. Effect of pump plunger area.

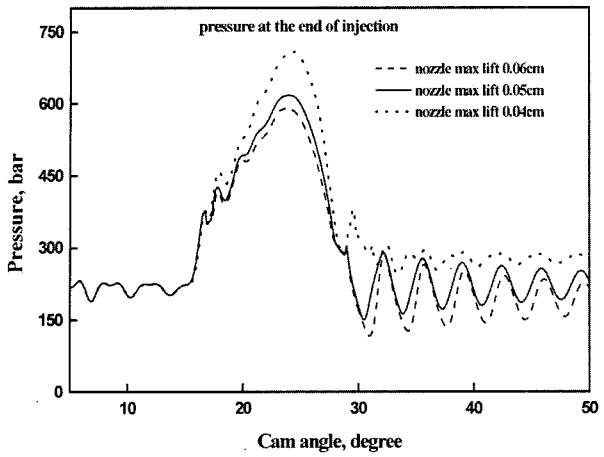

Figure 8. Effect of nozzle maximum lift.

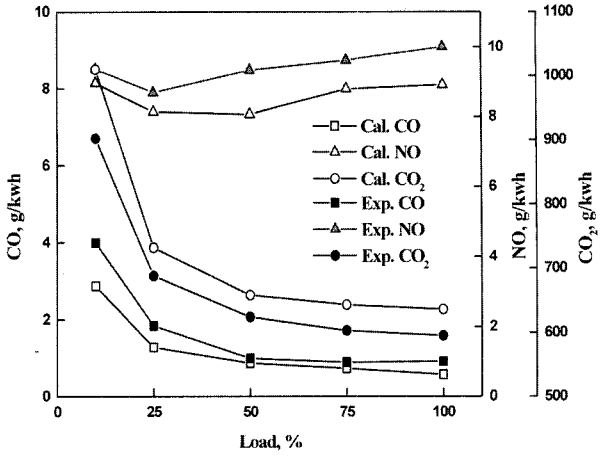

Figure 10. Comparison for experiment and calculation.

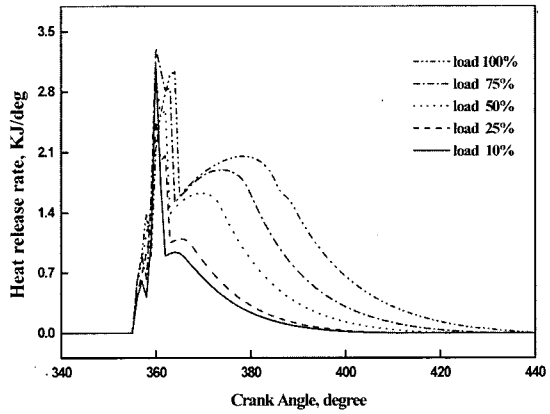

Figure 9. Prediction of ROHR with simulation.

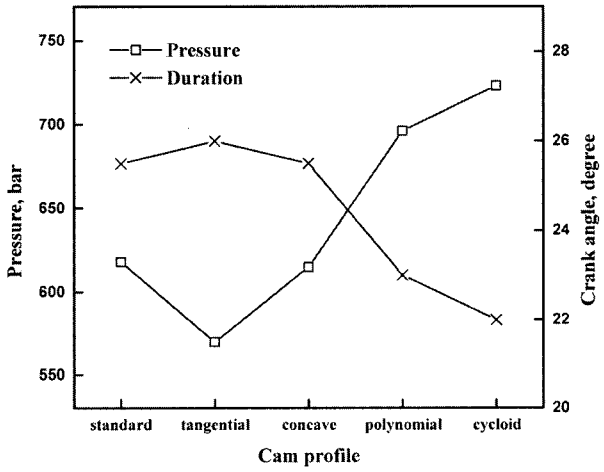

Figure 11. Effect of the calculated fuel injection pressure and duration for cam profile.

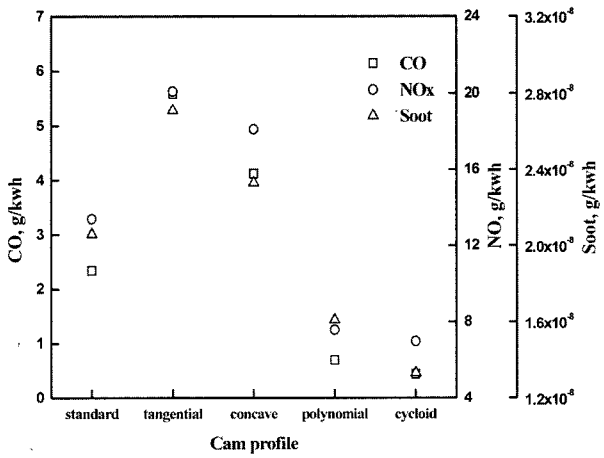

Figure 12. Effect of calculate emission for cam profile.

that combustion will be greatly affected by changes in plunger area, because the latter has a great impact on injection duration and injection flow. An increase in plunger area results in an increase in the pressure of the injection pipe, increasing main period of injection and injection flow. Figure 8 shows the effect of nozzle maximum lift on pressure: Fuel is not injected properly when the maximum lift of the needle valve is small, increasing the pressure within the injection pipe and causing secondary injection, which negativel affects the combustion process. Figure 9 shows the rate of heat release based on the variables returned from the injection rates that were calculated by the numerical model. The heat release that is calculated here will be a significant factor in calculating emissions due to combustion. Figure 10 shows the similarities between the experimental and calculated results. Figure 12 is the effect of calculated emissions due to different cam profile. In this study, it was expected to reduce exhaust emission more to apply polynomial or cycloid cam than to apply other cam. Because it is the shape of cam that decides plunger pumping speed and such pumping speed decides fuel injection rate together with fuel injection pressure. There-

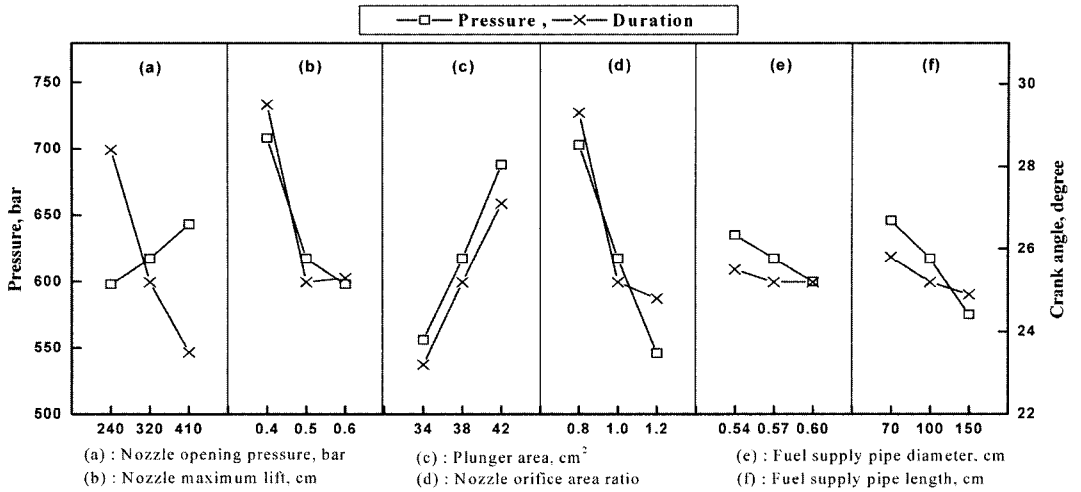

Figure 13. Effect of the calculated fuel injection pressures and durations with the parameters.

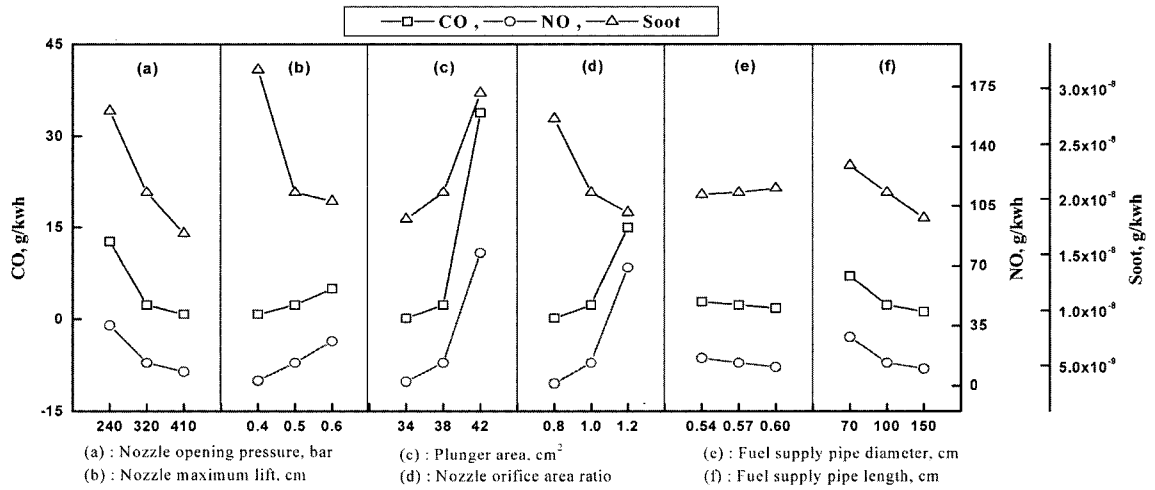

Figure 14. Effect of calculated emissions woth the parameters.

fore, concave and tangential cams reduce early injection rate and increase latter injection rate, but due to the stagnation of spray front, the penetration strength is weaken and combustion is badly affected. On the other hand, standard cam increases early injection rate, and large amount of fuel is burnt abruptly, as a result, increment of NO_X, accumulation of fuel in the air, prevention of uniform mixture occur. On the contrary, polynomial and cycloid cams can not only offer proper injection rate and uniform mixture but also they improve combustion condition by higher injection pressures as 696, 723 bar respectively comparing with other cams as shown in Figure 11. There is a suggestion here that the polynomial and cycloid cam can be seen as the shape of cam which decides appropriate fuel injection delay and plunger pumping speed compare with other cam. Figure 14, like Figure 12 also shows the prediction of exhaust emission. In Figure 14(a), changes in nozzle opening pressure affect the fuel injection duration and pressure as shown in Figure 13. Accordingly, when nozzle opening pressure is lower, fuel injection timing is faster and fuel injection duration is larger, and if nozzle opening pressure is higher, a large amount of fuel is injected at a time and thus not only combustion pressure but injection pressure becomes high, so that the development of atomization is promoted, the combination of atomizing fuel and air becomes harmonious and thus combustion is made good. Like this, as the density of spray becomes high, soot and *CO* are reduced and *NO* does not increase by high temperature but reduce by the shortage of combustion duration at the control combustion process. Figure 14(b) shows the results of nozzle maximum lift. If nozzle maximum lift is small, the fuel is not appropriately exhausted and thus a small amount of fuel is

burned, which may cause secondary injection and has an unfavorable effect on combustion by rising the pressure in the injection pipe, so that soot increases. Also, when nozzle maximum lift increase, fuel is injected so much, so that the temperature of combustion is high that adverse phenomenon appears. The figure shows the trade-off relation between *NO* and soot. On Figure 13, when nozzle maximum lift is as 0.4 cm, injection pressure is seemed, at first glance, to be high enough as 708 bar to improve combustion, but secondary injection have bad influence on condition. Figure 14(c) shows the effect due to change the plunger area. The plunger area determines the period of injection duration and amount, and pressure as shown in Figure 13, if the plunger area increases, the velocity of fuel pressure wave also increase, so as the injection timing leads, the premixed combustion becomes large, and as a result, *CO* and *NO* also rapidly increase. Especially, on Figure 13, when plunger area is as 42 cm^2, the injection pressure is relatively high as 688 bar. Although it is enough to improve combustion condition and to reduce emissions, soot is increased according to increase combustion duration. moreover, because large amount of fuel is burnt and cylinder gas temperature is higher, thermal dissociation is increased. And on the conclusion, both NO and CO increase abruptly. Figure 14(d) shows the effects of change in nozzle orifice area ratio, and similar to results shown in Figure 14(b), and is related to the fuel amount injected. In Figure 14(e) like Figure 13, the effect according to the change in the diameter of injection pipe does not show large change. Figure 14(f) shows the effect according to the change in the length of injection pipe, it is estimated that if the length of injection pipe increase, the injection delay becomes larger, thus the rise of combustion pressure delays and the gas temperature in cylinder relatively becomes low. On the contrary, when the length of injection pipe decrease, the injection delay leads, the combustion duration decreases, so that fuel injection is unfavorable and it influences badly in combustion. But, it has little effect comparing with other variables. Investigating in Figure 14, although NO_X and soot are generally on trade-off tendency, (a) and (c) show to have opposite trend. This is, as previously stated, originated from the different aspects which increase injection pressure and duration according to increasing variables. And, among the emissions calculated by several variables, except the effect by secondary injection of (b) and (d), (a) and (c) have larger effects, and (e) and (f) have relatively little effects.

5. CONCLUSIONS

The following conclusion were reached after performing simulations on a marine diesel engine fuel injection system and its emission.

(1) The results of fuel injection simulation were very similar to the results of actual experiment.
(2) Specific emission characteristics due to variations in the injection system were obtained via simulation and showed agreement with theory.
(3) In the injection system of this study, it can be predicted that polynomial and cycloid cam can not only offer proper injection rate and uniform mixture but also they improve combustion condition by higher injection pressure as 79 to 153 bar comparing with other cam.
(4) It is proper for the purpose of reducing the exhaust emission to increase the nozzle opening pressure if possible.
(5) It turned out that the nozzle maximum lift and nozzle orifice area are related to the fuel amount injected and pressure in injection pipe, and as a result, has a bad effect on combustion in case of reduce and if increase, soot is reduced.
(6) If the plunger area is increased in oder to raise the engine output, the fuel injection timing leads due to increase fuel pressure wave, so that the injection duration and injection amount increase, which results in increase in emission.
(7) There are no great changes in emission according to the change in the diameter of fuel injection pipe and the length of fuel injection pipe.
(8) Although NO_X and soot are generally on trade-off tendency, the effects by the variables of nozzle opening pressure and plunger area show to have opposite trend. This is originated from the different aspects which increase injection pressure and duration according to increasing variables.
(9) Among the emissions calculated by several variables, except the effect by secondary injection for the variables of nozzle maximum lift and nozzle orifice area, the variables of nozzle opening pressure and plunger area have larger effects, and the variables of fuel pipe diameter and length have relatively little effects.

REFERENCES

Bazari, Z. (1992). A DI diesel combustion and emission predictive capability for use in cycle simulation. *SAE Paper No.* 920462.

Becchi, G. A. (1971). Analytical simulation of fuel injection in diesel engines. *SAE Paper No.* 710568.

Dow, R. S and Fink, C. E. (1940). Computation of some physical properties of lubricating oils at high pressure. *Journal of Applied Physics* **2**.

Ham, Y. Y. and Chun, K. M. (2002). Parametric study for reducing NO and soot emissions in a DI diesel engine

by using engine cycle simulation. *Trans. Korean Society of Automotive Technology* **10, 5,** 35–44.

Hiroyasu, H. (1982). Diesel engine combustion and its modeling. Department of Mechanical Engineering University of Hirosima.

Kumar, K. (1983). A finite difference scheme for the simulation of a fuel injection system. *SAE Paper No.* 831337.

Mastuoka, S. (1976). A study of fuel injection systems in diesel engine. *SAE Paper No.* 760551.

Oh, S. K. Baik, D. S. and Han, Y. C. (2003). Emission characteristics in ultra low sulfur diesel. *Int. J. Automotive Technology* **4, 2,** 95–100.

Ohyama, Y. (2001) Engine control using combustion model. *Int. J. Automotive Technology* **2, 2,** 53–62.

Whitehouse, N. D. and Way, R. (1969–1970) Rate of heat release in diesel engines and its correlation with fuel injection data. *Proc Instn Mech Engrs.*

Wylie, E. B., Bolt, J. A. and El-Erian, M. F. (1971). Diesel fuel injection system simulation and experimental correlation. *SAE Paper No.* 710509.